Skeletal Radiology (2019) 48:1323–1328
https://doi.org/10.1007/s00256-019-3165-z

REVIEW ARTICLE

Progressive pseudorheumatoid dysplasia: a report of three cases and a review of radiographic and magnetic resonance imaging findings

Christy B. Pomeranz[1] · Janet R. Reid[2]

Received: 6 August 2018 / Revised: 11 January 2019 / Accepted: 16 January 2019 / Published online: 2 February 2019

Abstract
Progressive pseudorheumatoid dysplasia (PPD) is a rare disorder of postnatal skeletal and cartilage development that often presents with similar clinical findings to juvenile idiopathic arthritis. Patients with PPD display findings of progressive cartilage loss and secondary osteoarthritis over serial imaging studies and have an absence of elevation of inflammatory markers. Awareness of the imaging features of PPD on radiographs and magnetic resonance imaging (MRI) may be important for early diagnosis and surveillance of the disease.

Keywords Progressive pseudorheumatoid dysplasia · Skeletal dysplasias · Juvenile idiopathic arthritis · Pediatric radiology · Pediatric musculoskeletal imaging · Magnetic resonance imaging

Introduction

Progressive pseudorheumatoid dysplasia (PPD) is a rare disorder of postnatal skeletal and cartilage development that was first described by Spranger et al. and Wynne-Davies et al. [1–3]. PPD poses a diagnostic challenge due its rarity, occurring in approximately ~ 1 in 1 million patients [4], as well as due its unusual clinical presentation and significant clinical and imaging overlap with other pediatric musculoskeletal disorders, such as juvenile idiopathic arthritis (JIA), Scheuermann's disease, and spondyloepiphyseal dysplasia. PPD occurs secondary to mutations in the *WISP3* gene and although diagnosis can be definitively made with genetic testing, patients often undergo imaging prior to genetic testing and the radiologist may play a crucial role in diagnosis at presentation as well as in follow-up of disease progression and its complications.

Here we review the imaging findings of PPD on both radiographs and cross-sectional imaging, with a special focus on musculoskeletal MRI, as well as examine the pitfalls in radiographic diagnosis in three patients from our institution (Table 1). Additionally, due to the dearth of information on the features of PPD on musculoskeletal MRI, we discuss the possible role and utility of MRI in these patients.

Genetic and molecular considerations

The majority of cases of progressive pseudorheumatoid dysplasia (PPD; MIM 208230) are familial, often occurring in families with a history of consanguinity with two-thirds of cases occurring in patients of Arab descent [5, 6]. PPD is due to mutations in the *WISP3* gene and displays an autosomal recessive inheritance pattern. The *WISP3* gene encodes a protein in the connective tissue growth factor (CTGF) family that is expressed in synoviocytes and chondrocytes and plays a major role in bone and cartilage growth and development [7]. In fact, biopsies of the iliac crests in patients with PPD have shown that the chondral surface is the primary location of pathology, demonstrating abnormal nest-like clustering of chondrocytes in the chondral rests and marked deficiency in cartilage growth [8, 9].

Clinical presentation and differential diagnosis

Patients with PPD are normal at birth and in infancy. The main clinical features of PPD do not begin to manifest

✉ Christy B. Pomeranz
christypomeranz@gmail.com

[1] Department of Radiology, New York-Presbyterian Hospital/Weill Cornell Medicine, 525 E. 68th St., F631E, New York, NY 10065, USA

[2] Department of Radiology, The Children's Hospital of Philadelphia, 34th Street & Civic Center Boulevard, Philadelphia, PA 19104, USA

Table 1 Patients with Progressive Pseudorheumatoid Dysplasia

Patient	Age at diagnosis	Gender	Inflammatory markers	Genetics	Clinical presentation	Images
1	10 years	F	ESR 16 CRP < 0.5 RF negative	*WISP3* homozygous	Short stature, genu valgum, and difficulty walking. Misdiagnosed as Legg–Calvé–Perthes disease	Fig. 1 radiographs Fig. 2 MRI of the hip
2	10 years	F	ESR 14 CRP < 0.05 RF negative	*WISP3* homozygous	Joint pain. Misdiagnosed as JIA at age 4; treated with Enbrel without improvement	Figs. 3 and 5 radiographs Figs. 4 and 6 MRI of the ankle and shoulder
3	8 years	M	ESR 17 CRP 1.0 RF negative	*WISP3* compound heterozygous on exon 3 and exon 4	Morning stiffness and back soreness; confined to a wheelchair. Misdiagnosed as bilateral SCFE, right-sided Blount's and congenital coxa vara	Fig. 3 radiographs

until 3–6 years old, with an age range of 1–16 years being reported in the literature [6, 10]. Presenting symptoms typically include joint pain and stiffness, joint contractures, enlarged metacarpophalangeal (MCP) and interphalangeal joints (IP), gait abnormalities, and short stature [11, 12]. Initially, patients with PPD demonstrate normal height but as skeletal manifestations progress, they begin to demonstrate short stature with heights under the third percentile [4].

There is significant clinical overlap with JIA due to the pain and swelling in multiple joints but, unlike in JIA, there is no elevation of inflammatory markers and serum is negative for rheumatoid factor, which may help to clinically differentiate the two diseases. Initial imaging performed may also demonstrate imaging overlap with JIA, spondyloepiphyseal dysplasia tarda, and Scheuermann's kyphosis. In our cohort, patients not only presented with diffuse joint pain leading to a misdiagnosis of JIA, but also presented with a series of other joint specific abnormalities (Table 1). Two patients demonstrated femoral head abnormalities misdiagnosed as Legg–Calvé–Perthes disease and slipped capital femoral epiphysis.

Imaging

Radiographs are often the first-line modality of imaging in patients with PPD and demonstrate diffuse osteopenia and multiple skeletal abnormalities, often centered at the joint or chondral surface, raising suspicion for a skeletal dysplasia or an inflammatory process. There are signs of a secondary osteoarthritis in all visualized joints, including joint space narrowing, osteophyte formation, and peri-articular osteopenia. There is also diffuse demineralization of the bones, predisposing patients to fractures (Figs. 4d and 5).

Magnetic resonance imaging (MRI) is currently not routinely used in the work-up or diagnosis of PPD. Therefore, little has been previously described in the literature with regard to MRI findings in the setting of PPD. There are several MR images of the spine depicted in both the radiology and

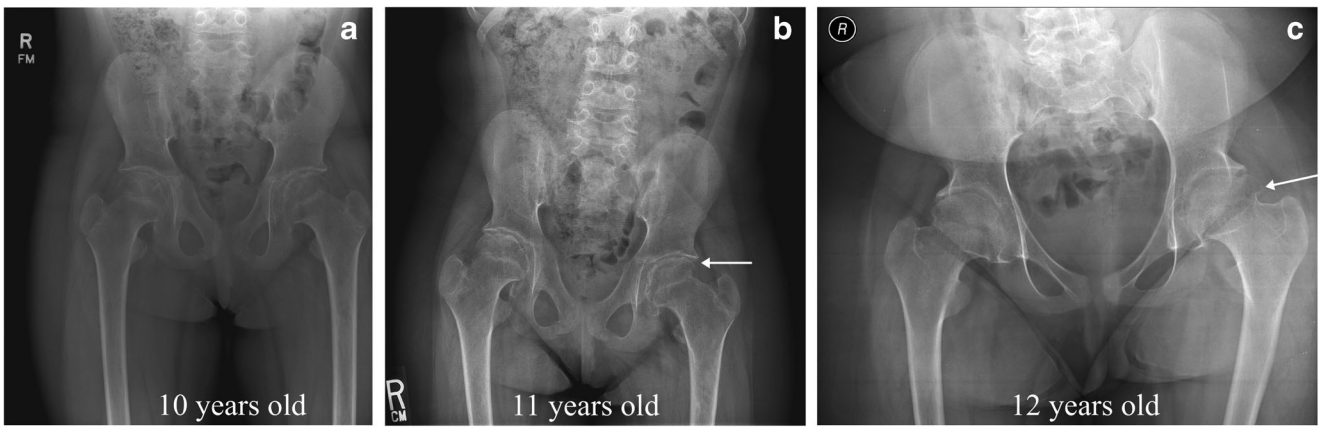

Fig. 1 Frontal radiograph of the pelvis in patient 1 at **a** 10 years old, **b** 11 years old, and **c** 12 years old demonstrates coxa magna and coxa vara deformities of the proximal femurs and progressive joint space narrowing, subchondral irregularity, and osteophyte formation. More advanced stages show mild femoral head flattening (*arrows*)

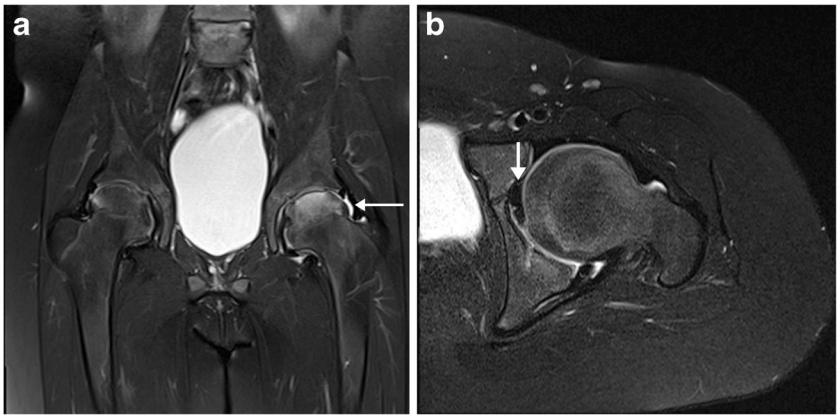

Fig. 2 Patient 1. **a** Coronal STIR sequences of the hips demonstrate marked joint space narrowing of both hip joints, with left greater than right. There is coxa magna and coxa vara deformities of the bilateral proximal femurs. In the left femoral head, there is flattening and reactive bone marrow edema (*thin arrows*). **b** Axial T2-weighted fat-saturated sequences of the left hip demonstrates marked cartilage loss over the entire left femoral head and joint space narrowing. There is hypertrophy of the ligamentum teres (*bold arrow*)

rheumatology literature [13–16], however, only a single musculoskeletal MR image currently exists in the rheumatology literature [16] and none have yet to be published in the radiology literature. Moreover, MRI may be an important modality in these patients, as it provides better delineation of the primary site of pathology—the articular cartilage—which is radiographically invisible. The imaging findings of PPD on musculoskeletal MRI tend to be more specific and are less likely to demonstrate overlap with JIA. Specifically, MRI demonstrates an absence of an inflammatory process—no

Fig. 3 Patient 2 and patient 3. **a**, **b** Frontal radiographs of the feet demonstrate peri-articular osteopenia and enlargement of the metaphyses at the MTP and IP joints with joint space narrowing. **c**, **d** Lateral views of the bilateral ankles in the same patient at age 10 demonstrate fusion of an enlarged os trigonum with the posterior talus (*thin arrows*). There is also osteopenia and early degenerative changes at the tibiotalar joints (*bold arrows*)

articular or periarticular erosions, no large joint effusions or synovitis, no pannus formation or surrounding soft tissue edema is present—as is seen in the setting of the JIA. MRI of several large joints—including the hip, shoulder, and ankle—have been performed at our institution and have demonstrated a myriad of findings supporting the diagnosis of PPD.

Serial radiographs of the hips and pelvis were performed on patient 1. In the early stages of PPD, radiographs demonstrated a coxa vara deformity of the proximal femurs and marked enlargement of the proximal femoral epiphyses (coxa magna) (Fig. 1a). In later stages, there were findings of osteoarthritis, including joint spacing narrowing, osteophyte formation and subchondral cyst formation in the femoral head and acetabulum (Fig. 1b, c) [13]. In the advanced stages, there was progressive arthritis with joint space narrowing and mild femoral head flattening mimicking Legg–Calvé–Perthes disease, which was the initial misdiagnosis in this patient (Fig. 1b, c). MRI of the hip in this same patient demonstrated similar findings to radiographs, including enlargement of the femoral head epiphysis (coxa magna), coxa vara, and joint space narrowing (Fig. 2a, b). However, MRI also demonstrated a number of additional radiographically occult findings including diffuse thinning of the articular cartilage over the entire femoral epiphysis and subcortical irregularity (Fig. 2b). There was also reactive bone marrow edema in the femoral epiphysis and a small joint effusion (Fig. 2a), which was not visualized on radiographs and likely due to friction from bone-on-bone apposition rather than a primary inflammatory process. Altered biomechanics also resulted in abnormal appearance and thickening of stabilizing structures on the hip, such as the ligamentum teres (Fig. 2b). Finally, MRI did not show findings of Legg–Calvé–Perthes disease, which had been

Fig. 4 Patient 2. **a** Sagittal T1-weighted image of the right ankle demonstrates diffuse cartilage loss at the tibiotalar (*bold arrows*) and subtalar joints (*thin arrows*) with joint space narrowing and osteophyte formation. **b** Sagittal STIR demonstrates marked deformity of the talus and an erosion at the talar neck (*thin arrows*), likely related to impingement. **c** Coronal T1-weighted sequence shows thickening of the calcaneofibular ligament (*bold arrow*). **d** Footprint STIR sequence of the midfoot demonstrates a stress fracture of the first metatarsal

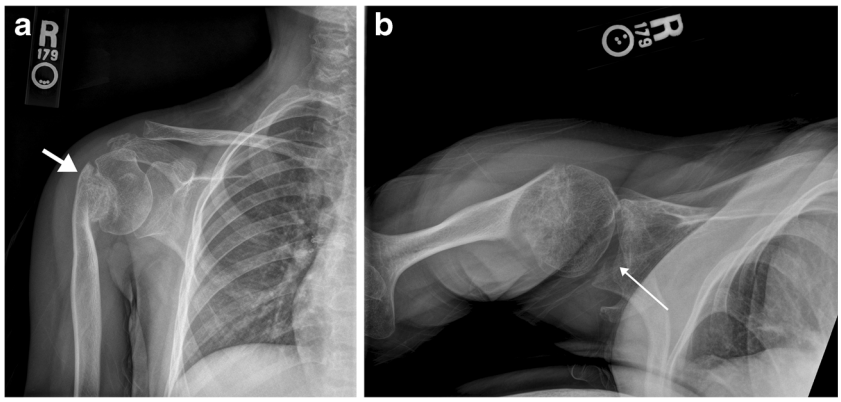

Fig. 5 Patient 2. **a**, **b** Frontal and axillary views of the shoulder demonstrate glenohumeral joint space narrowing and subchondral irregularity of the glenoid (*thin arrow*). There is a chronic fracture deformity of the proximal humeral metaphyses (*bold arrow*)

suggested on the prior radiographs. Thus, MRI allowed for better delineation of the findings of a secondary osteoarthritis in this patient—including joint space narrowing, early or small osteophyte formation and a lack of articular and periarticular erosions [16]. MRI of the hip may also be helpful in evaluation of the labrum in patients with PPD as these patients may be prone to degenerative labral tears at an earlier age, much like in adult patients with primary osteoarthritis and long-standing chondral wear.

Radiographs of the feet and ankle were performed in patients 2 and 3. Radiographic sequela of PPD in these patients included severe osteopenia, broadening of the small tubular bones of the feet, widening of distal metaphyses of the proximal phalanges, and enlargement of the epiphyses of the metatarsals (Fig. 2a and b). Radiographs of the ankle also showed tibiotalar joint space narrowing as well as an enlarged or mega os trigonum with fusion to the talus; this finding has been previously described in the literature and may also further help to differentiate from JIA (Fig. 2c, d) [14, 17]. MRI of the ankle in patient 2 further delineated findings of a secondary osteoarthritis at the tibiotalar and subtalar joints where is there is marked joint space narrowing and osteophyte formation. However, MRI also showed diffuse loss of articular cartilage at both the tibiotalar and subtalar joints, as well diffuse cartilage loss throughout the midfoot articulations (Fig. 4a, b), which was not well seen on radiographs. In our example, MRI was also useful at detecting a small erosion and osteophyte at the talar neck near the anterior tibiotalar joint capsule, likely related anterior impingement (Fig. 4b). As with the supporting structures of the hip, there was also thickening of the ankle ligaments likely reflecting altered biomechanics, as is seen involving the calcaneofibular ligament (Fig. 4c). There were scattered signal abnormalities throughout the bone marrow due to osteopenia and a stress fracture of the first metatarsal, which was radiographically occult and likely related to altered biomechanics and osteopenia (Fig. 4d).

Patient 2 also underwent imaging of the shoulder. On radiographs, there was chronic fracture deformity of the proximal humeral metaphysis as well marked joint space narrowing and subchondral irregularity at the glenohumeral joint (Fig. 5a and b). MRI of the shoulder demonstrated similar abnormalities to the other large joints with recurrent findings of a secondary osteoarthritis and an absence of inflammatory signs such as soft tissue edema, synovitis, and pannus formation (Fig. 6a, b). MRI of the shoulder also provided improved visualization of the articular cartilage of the humeral epiphysis

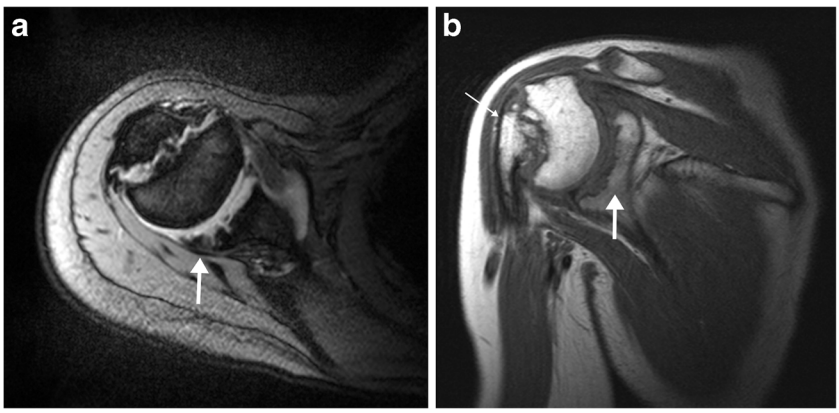

Fig. 6 Patient 2. **a** Axial T2 GRE of the right shoulder demonstrates diffuse cartilage loss over the humeral head and severe cartilage loss over the posterior glenoid, where there is marked subchondral irregularity and fragmentation (*bold arrow*). There is joint space narrowing. **b** Coronal T1-weighted image demonstrates joint space narrowing and marked subchondral irregularity of the glenoid (*bold arrows*). There is a chronic Salter–Harris type II fracture involving the proximal physis and metaphysis of the humerus (*thin arrows*)

and glenoid where there was diffuse chondral loss at the epiphysis and severe chondral loss and subchondral irregularity along the posterior glenoid (Fig. 6a, b). This pattern of chondral loss and irregularity at the posterior glenoid is similar to findings seen in adult patients with primary osteoarthritis and, much like adult patients with primary osteoarthritis, these patients may also be prone to degenerative tears of the glenoid labrum, which MRI may be helpful in delineating.

Thus, MRI may be useful for helping distinguish PPD from its clinical and radiographic mimic, JIA, by demonstrating a lack of an inflammatory process with an absence of soft tissue edema, synovitis, and pannus formation. MRI of the hip may also be useful to exclude Legg–Calvé–Perthes disease in the setting of femoral head flattening. Finally, there may also be a role for MRI in evaluating the non-osseous findings in PPD, such as cartilage loss and degenerative tears of glenoid and/or labrum, and for evaluating for radiographically occult stress fractures due to underlying osteopenia. The drawbacks of MRI include the increased expense and possible need for sedation in young children. Therefore, MRI should not be used as a screening modality in PPD.

Conclusions

In conclusion, PPD is a very rare genetic disorder characterized by marked deficiency of the articular cartilage and progressive changes of secondary osteoarthritis with a clinical presentation in childhood that may mimic JIA without elevation of inflammatory markers. Radiographs are non-specific and can be confused with other disorders including JIA. Musculoskeletal MRI best depicts the characteristic findings of diffuse cartilage loss and lack of an inflammatory process—prompting genetic confirmation of PPD over JIA—and can be very helpful in assessing the degree of cartilage loss and associated complications of PPD.

References

1. Spranger J, Albert C, Schilling F, Bartsocas C, Stöss H. Progressive pseudorheumatoid arthritis of childhood (PPAC)—a hereditary disorder simulating rheumatoid arthritis. Eur J Pediatr. 1983;140(1):34–40.
2. Spranger J, Albert C, Schilling F, Bartsocas C. Progressive pseudorheumatoid arthropathy of childhood (PPAC): a hereditary disorder simulating juvenile rheumatoid arthritis. Vol. 14, American journal of medical genetics. New York: Liss; 1983. p. 399–401.
3. Wynne-Davies R, Hall C, Ansell BM. Spondylo-epiphysial dysplasia tarda with progressive arthropathy. A "new" disorder of autosomal recessive inheritance. Vol. 64, the journal of bone and joint surgery - British volume. London: British Editorial Society of Bone and Joint Surgery; 1982. p. 442–5.
4. Bhavani GSL, Shah H, Shukla A, Dalal AGK. Progressive Pseudorheumatoid dysplasia. In: Adam M, Ardinger H, Pagon R, editors. GeneReviews [Internet]. Seattle (WA): University of Washington, Seattle; 2015.
5. el-Shanti HE, Omari HZ, Qubain HI. Progressive pseudorheumatoid dysplasia: report of a family and review. Journal of medical genetics London : British Medical Association; 1997. 34:559–63.
6. Ekbote AV, Danda D, Kumar S, Danda S, Madhuri V, Gibikote S. A descriptive analysis of 14 cases of progressive-psuedorheumatoid-arthropathy of childhood from South India: review of literature in comparison with juvenile idiopathic arthritis. Vol. 42, seminars in arthritis and rheumatism. Philadelphia: WB Saunders; 2013. p. 582–9.
7. Sailani MR, Chappell J, Jingga I, Narasimha A, Zia A, Lynch JL, et al. *WISP3* mutation associated with pseudorheumatoid dysplasia. Vol. 4, Cold Spring Harbor molecular case studies. Cold Spring Harbor: Cold Spring Harbor Laboratory Press; 2018.
8. Hurvitz JR, Suwairi WM, Van Hul W, El-Shanti H, Superti-Furga A, Roudier J, et al. Mutations in the CCN gene family member *WISP3* cause progressive pseudorheumatoid dysplasia. Vol. 23, nature genetics. New York: Nature Pub Co; 1999. p. 94–8.
9. Legius E, Mulier M, van Damme B, Fryns JP. Progressive pseudorheumatoid arthritis of childhood (PPAC) and normal adult height. Clin Genet. 1993;44(3):152–5.
10. Delague V, Chouery E, Corbani S, Ghanem I, Aamar S, Fischer J, et al. Molecular study of *WISP3* in nine families originating from the middle-east and presenting with progressive pseudorheumatoid dysplasia: identification of two novel mutations, and description of a founder effect. Vol. 138A, American journal of medical genetics. Hoboken: Wiley-Liss; 2005. p. 118–26.
11. Wickrematilake G. Progressive Pseudorheumatoid Dysplasia or JIA? Case Rep Rheumatol [Internet]. 2017;2017(Figure 1):1–3. Available from: https://www.hindawi.com/journals/crirh/2017/1609247/
12. Teebi AS, Al Awadi SA. Spondyloepiphyseal dysplasia tarda with progressive arthropathy: a rare disorder frequently diagnosed among Arabs. J Med Genet. 1986;23(2):189–91.
13. Mampaey S, Vanhoenacker F, Boven K, Hul W, Van de Schepper A. Progressive pseudorheumatoid dysplasia. Eur Radiol. 2000;10(11):1832–5.
14. Kaya A, Ozgocmen S, Kiris A, Ciftci I. Clinical and radiological diagnosis of progressive pseudorheumatoid dysplasia in two sisters with severe polyarthropathy. Vol. 24, clinical rheumatology. Brussels: Acta Medica Belgica; 2005. p. 560–4.
15. Gao YS, Ding H, Zhang CQ. Total hip arthroplasty in a 17-year-old girl with progressive pseudorheumatoid dysplasia. J Clin Rheumatol. 2013;19(3):138–41.
16. Ehl S, Uhl M, Berner R, Bonafé L, Superti-Furga A, Kirchhoff A. Clinical, radiographic, and genetic diagnosis of progressive pseudorheumatoid dysplasia in a patient with severe polyarthropathy. Rheumatol Int. 2004;24(1):53–6.
17. Oestreich AE. Mega os trigonum in progressive pseudorheumatoid dysplasia. Vol. 32, Pediatric radiology. Berlin: Springer-Verlag; 2002. p. 46–8.